Local impurity effects in superconducting graphene

T. O. Wehling,[1] H. P. Dahal,[2] A. I. Lichtenstein,[1] and A. V. Balatsky[2,3,∗]

[1]*I. Institut für Theoretische Physik, Universität Hamburg, Jungiusstraße 9, D-20355 Hamburg, Germany*
[2]*Theoretical Division, Los Alamos National Laboratory, Los Alamos, New Mexico 87545,USA*
[3]*Center for Integrated Nanotechnologies, Los Alamos National Laboratory, Los Alamos, New Mexico 87545,USA*
(Dated: February 1, 2008)

We study the effect of impurities in superconducting graphene and discuss their influence on the local electronic properties. In particular, we consider the case of magnetic and non-magnetic impurities being either strongly localized or acting as a potential averaged over one unit cell. The spin dependent local density of states is calculated and possibilities for visualizing impurities by means of scanning tunneling experiments is pointed out. A possibility of identifying magnetic scatters even by non spin-polarized scanning tunneling spectroscopy is explained.

Graphene - one monolayer of carbon atoms arranged in a honeycomb lattice - can be considered as one of the most promising materials for post-silicon electronics [1]. Impurity states often are the basis of modern electronic devices. Because of its peculiar electronic structure graphene provides a model system for studying relativistic quantum physics in condensed matter [2, 3]. A careful investigation of the impurity states in graphene also allows one to address fundamental questions of relativistic scattering [4–8]. Thus, far the central component to these studies is graphene's linearly vanishing density of states (DOS) near the Dirac point: It allows for virtual bound states (VBS) in this region, i.e. resonances in the DOS, which may be arbitrarily sharp in the vicinity of the Dirac point. The broad similarities of these impurity states with states in d-wave superconductors have been used to discuss common aspects of impurity scattering in superconductors and in graphene [5, 6, 8–10].

Recently, it has been demonstrated that it is possible to induce superconductivity in graphene via a proximity effect [11]. Prior analysis of the ballistic superconducting transport [12] revealed an interesting suppression of the critical current near the Dirac point. It is therefore simply a matter of time before the defects and impurity induced states in superconducting graphene will be addressed locally. The case of superconductivity in graphene where opposite valleys are nontrivially involved is also an explicit example of supercondcutivity in vallyetronics [13]. The observation of the proximity effect in graphene raised fundamentally new questions about impurity effects in this material in presence of superconducting correlations: i) Is there a possibility of intragap bound states and ii) what is the impact of gap opening on the Friedel oscillations in the continuum?

In this letter we show that magnetic impurities do produce impurity bound states *inside the superconducting gap*. These bound states *always* coexist with the formerly studied VBS in the continuum. Thus the predicted impurity states are similar to the magnetic impurity induced states, so called Yu Lu-Shiba-Rusinov states, in s-wave superconductors [9, 14]. Due to its 2 dimensionality graphene is well suited for Scanning Tunneling Mi-

croscopy (STM) investigations and first experiments on normal state graphene already indicate the importance of impurity effects in this context [15, 16]. Therefore, we elucidate the real space shape of these impurity states, which will be directly observable in STM experiments.

While graphene intrinsically is not superconducting, the Ti/Al bilayer contacts placed on the graphene sheet induce a measured supercurrent [11]. No spectral gap in the samples has been measured to date. We argue that the residual electron-electron interaction in the graphene will produce a *gap* in the spectrum. This gap will be proportional to the interaction strength and it remains to be seen how large this gap can be in the graphene. Electron spectroscopy such as STM and/or planar tunneling into graphene in proximity to superconducting leads would be able to reveal the spectroscopic gap. We will treat superconducting gap Δ below as a phenomenological parameter that needs to be determined separately.

Low energy electronic excitations in graphene can be described by two species of Dirac fermions located around two nodal points $K^{\pm}$ in the Brillouin zone with the speed of light being replaced by the Fermi velocity $v_{\rm f}$ and the corresponding Hamiltonian $H_{K^{\pm}} = v_{\rm f}\hbar(k_1\sigma_1 \mp k_2\sigma_2)$. σ_i, $i = 1, 2, 3$, are Pauli matrices acting on the sublattice degrees of freedom and σ_0 is the identity matrix. To understand impurities in superconducting graphene, we use the Nambu formalism including both valleys:

$$\hat{H} = -i\hbar v_f \int \mathrm{d}^2x \hat{\Psi}^\dagger(x)(\partial_1\sigma_1\otimes\tau_0 - \partial_2\sigma_2\otimes\tau_3)\otimes\Lambda_0\hat{\Psi}(x)$$

with $\hat{\Psi}(x)^\dagger = (\Psi^\dagger_{\downarrow K^+}(x), \Psi^\dagger_{\downarrow K^-}(x), \Psi_{\uparrow K^-}(x), \Psi_{\uparrow K^+}(x))$ and $\Psi_{\uparrow\downarrow K^\pm}(x)$ being field operators of electrons with a spin $\uparrow\downarrow$ and belonging to a valley $K^\pm$. τ_i and Λ_i with $i = 1, 2, 3$ are Pauli matrices but acting on the valley and Nambu space, respectively. τ_0 and Λ_0 are the corresponding identity matrices. In contact with a superconductor, the proximity effect imposes a finite pairing potential $\Delta\sigma_3 \otimes \tau_0 \otimes \Lambda_1$ to the graphene sheet and results in electron dynamics being described by the Dirac-Bogoliubov-de Gennes (DBdG) Hamiltonian [17]:

$$H = -i\hbar v_f(\partial_1\sigma_1\otimes\tau_0 - \partial_2\sigma_2\otimes\tau_3)\otimes\Lambda_0 + \Delta\sigma_3\otimes\tau_0\otimes\Lambda_1. \quad (1)$$
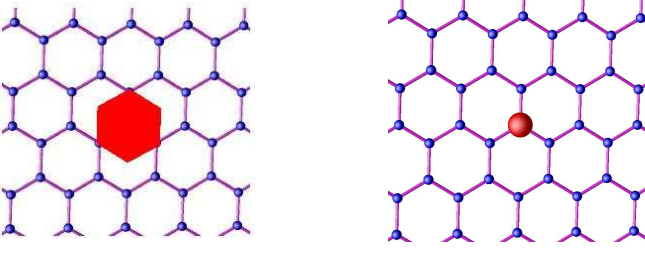
arXiv:0704.3115v1 [cond-mat.mes-hall] 24 Apr 2007

Figure 1: (Color online) Among the various local impurities we discuss two limiting cases. The scalar impurity (left), V_s, corresponds to a uniform potential averaged over one unit cell, whereas the on-site impurity (right), V_o, acts on one sublattice only.

To elucidate the effect of different impurities, we discuss both, a homogeneous potential acting within one unit cell V_s (referred to as scalar impurity, Fig. 1.a) as well as a strongly localized impurity V_o (referred to as on-site impurity, Fig. 1.b) acting only at sublattice A and giving rise to intervalley scattering.

Starting from impurity operators in the tight-binding form of e.g. Ref. [8] and using the conventions of Eqn.

(1) we obtain the following explicit expressions for the impurity potentials in the adopted matrix notation: $V_s = V_0\sigma_0 \otimes \tau_0 \otimes \Lambda_3 + V_1\sigma_0 \otimes \tau_0 \otimes \Lambda_0$ and $V_o = V_0(\sigma_3 + \sigma_0) \otimes (\tau_0 + \tau_1) \otimes \Lambda_3 + V_1(\sigma_3 + \sigma_0) \otimes (\tau_0 + \tau_1) \otimes \Lambda_0$ [18]. In both cases V_0 and V_1 describe the electrostatic and magnetic contribution to the impurity potential, respectively.

The effects of these impurities on the local electronic properties of the superconducting graphene sheets is contained in the local density of states (LDOS), which we calculate using the T-matrix approach [9]: In operator form, the full Green's function $G(\omega)$ in presence of the impurity is obtained from the unperturbed Green's function $G^0(\omega)$ via $G(\omega) = G^0(\omega) + G^0(\omega)T(\omega)G^0(\omega)$ with $T(\omega) = V_{s(o)}(1 - G^0(\omega)V_{s(o)})^{-1}$.

Dealing with local impurities, it is convenient to adopt the position space representation. Therefore, the free x-dependent Green's function $\hat{G}^0(x,\omega)$ in polar coordinates, $x = x(r,\phi)$, is obtained from its momentum space counterpart $\hat{G}^0(p,\omega) = (\omega - H)^{-1} = \frac{(\omega\sigma_0 \otimes \tau_0 + v_f[p_1\sigma_1 \otimes \tau_0 - p_2\sigma_2 \otimes \tau_3]) \otimes \Lambda_0 + \Delta\sigma_3 \otimes \tau_0 \otimes \Lambda_1}{\omega^2 - v_f^2 p^2 - \Delta^2}$ by Fourier transformation

$$\hat{G}^0(x,\omega) = \int \frac{d^2p}{\Omega_B} \hat{G}^0(p,\omega)e^{ipx} = g_0(r,\omega)(\omega\sigma_0 \otimes \tau_0 \otimes \Lambda_0 + \Delta\sigma_3 \otimes \tau_0 \otimes \Lambda_1) + g_1(r,\omega)([\cos\phi\,\sigma_1 \otimes \tau_0 + \sin\phi\,\sigma_2 \otimes \tau_3] \otimes \Lambda_0) \quad (2)$$

with $g_0(r,\omega) = v_f^2 \int_0^{p_c} dp\, p J_0(pr)(W^2(\omega^2 - \Delta^2 - v_f^2 p^2))^{-1}$ and $g_1(r,\omega) = iv_f^3 \int_0^{p_c} dp\, p^2 J_1(pr)(W^2(\omega^2 - \Delta^2 - v_f^2 p^2))^{-1}$, where we expressed the Brillouin zone volume $\Omega_B = 2\pi W^2/v_f^2$ in terms of the bandwidth W. The Green's function at $x = 0$ determines the LDOS of the free system and it occurs in the T-matrix: $\hat{G}^0(0, \omega + i\delta) = M(\omega)(\omega\sigma_0 \otimes \tau_0 \otimes \Lambda_0 + \Delta\sigma_3 \otimes \tau_0 \otimes \Lambda_1)$. Here is $M(\omega) = M'(\omega) + iM''(\omega)$ with $M'(\omega) = \frac{1}{2W^2}\ln\left|\frac{\Delta^2 - \omega^2}{W^2 + \Delta^2 - \omega^2}\right|$ and $M''(\omega) = -\frac{\pi\,\text{sgn}(\omega)}{2W^2}$ for $\Delta^2 < \omega^2 < \Delta^2 + W^2$ and $M''(\omega) = 0$ else. One sees, that the corresponding LDOS vanishes within the superconducting gap ($\omega^2 < \Delta^2$) and is given by $N_0(\omega) = \frac{4|\omega|}{W^2}$ outside the gap.

In general, impurity resonances occur when the T matrix becomes (almost) singular, i.e. $\det(1 - G^0(0,\omega)V) = 0$. For the scalar impurity this secular equation yields $1 - 2M(\omega)\omega V_1 + M^2(\omega)(\omega^2 - \Delta^2)(V_1^2 - V_0^2) = 0$ with solutions that can be understood analytically in the following limiting cases: Firstly consider a solely magnetic impurity, i.e. $V_0 = 0$, with $V_1 > 0$. In the Born limit the solutions $\omega_0 = -\Delta \pm \delta\omega$ with

$$\delta\omega = \frac{W^2}{2\Delta}e^{-W^2/(\Delta V_1)} \quad (3)$$

give rise to intragap bound and virtual bound states in

the continuum approaching the gap edge exponentially with decreasing V_1. In the opposite limit of unitary scattering $\omega_0 = \pm\Delta - \delta\omega$ with

$$\delta\omega = -\frac{2W^2}{V_1 \ln\left(\frac{2\Delta}{V_1}\right)} \quad (4)$$

fulfills the secular equation, where the upper (lower) sign corresponds to a intragap bound (continuum virtual bound) state.

The numerical solutions to energies of the intragap bound states are shown in Fig. 2. It recovers the limiting cases obtained analytically and demonstrates also the effect of an electrostatic contribution V_0 to the impurity potential: In the Born limit, the exponential dependence of $\delta\omega$ on the magnetic potential strength V_1 is dominant and suppresses any significant influence of V_0 on the impurity state energy. In the $V_1 \to \infty$ limit, V_0 leads to a renormalization of the *effective* magnetic potential strength $V_1 \to V_1(1 - \frac{V_0^2}{V_1^2})$. As Fig. 2 shows, the effect of an additional electrostatic potential becomes most pronounced in the intermediate region. There, the electrostatic contribution reduces the effective magnetic potential strength most significantly.
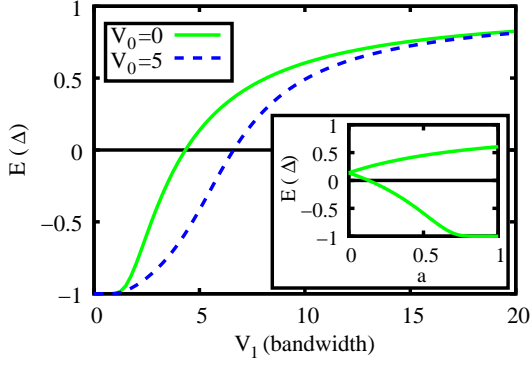
Figure 2: (Color online) Energy of the impurity resonance for the scalar impurity as a function of the magnetic impurity potential V_1 for different electrostatic potentials V_0. The gap-parameter is $\Delta = W/10$. The lower right inset shows the splitting of the impurity state due to intervalley scattering. We model intervalley scattering as $V = V_1(\sigma_0 \otimes \tau_0 \otimes \Lambda_0 + a\sigma_0 \otimes \tau_1 \otimes \Lambda_0)$ with the strength of the intervalley scattering parametrized by a and $V_1 = 5W$. One split state is shifted to the gap edge, the other state remains an intragap state.

Having understood the energy of intra gap bound states due to scalar impurities, we address now the strongly localized on-site impurities and elucidate the effect of inter valley scattering. Due to valley degeneracy, the scalar impurity gives rise to doubly degenerate intra gap bound states. This degeneracy is lifted by intervalley scattering, see Fig. (2). The secular equation corresponding to the on-site impurity, $1 - 8M(\omega)\omega V_1 + 16M^2(\omega)(\omega^2 - \Delta^2)(V_1^2 - V_0^2) = 0$, reduces to that of an on-site impurity with the replacement $V_{0,1} \to 4V_{0,1}$. Besides the lifting of the valley degeneracy, additional intervalley scattering results also in a renormalization of the effective impurity strength.

With the real-space Green's function $G(x, x', \omega) = G^0(x - x', \omega) + G^0(x, \omega)T(\omega)G^0(-x', \omega)$ one obtains the local density of states $N(x, \omega) = N_0(\omega) + \delta N(x, \omega) = -\frac{1}{\pi}\text{Im}G(x, x, \omega)$ in presence of an impurity. This LDOS is a matrix corresponding to the matrix structure of the Green's function. It accounts for the contributions from the different sublattices, valleys and the Nambu space. According to the convention in Eqn. (1), the spin-up excitations are hole excitations yielding for each spin component the LDOS $N_{\downarrow\uparrow}(x, \omega) = \text{Tr}\frac{\Lambda_0 \pm \Lambda_3}{2}N(x, \pm\omega)$, where the trace involves either the spin-down or up part of the Nambu space. In the case of the scalar impurity, this yields explicitly the following corrections to the unperturbed LDOS in the continuum

$$\delta N_{\downarrow\uparrow}(r, \pm\omega) = -\frac{4}{\pi}\text{Im}\frac{a_{\downarrow\uparrow}g_0^2(r, \omega) + b_{\downarrow\uparrow}g_1^2(r, \omega)}{1 - 2M(\omega)\omega V_1 + M^2(\omega)(\omega^2 - \Delta^2)(V_1^2 - V_0^2)} \quad (5)$$

with $a_{\downarrow\uparrow} = (\omega^2 - \Delta^2)[\pm V_0 + M(\omega)\omega(V_0^2 - V_1^2)] + (\omega^2 + \Delta^2)V_1$ and $b_{\downarrow\uparrow} = (\pm V_0 + V_1) + M(\omega)\omega(V_0^2 - V_1^2)$.

By replacing $M(\omega) \to 4M(\omega)$ in these formula, one obtains the case of the strongly localized on-site impurity. In STM experiments, graphene's lattice structure will give rise to a triangular modulation of the impurity states. This is neglected here, as similar effects in normal state graphene have been discussed in Ref. [8].

Due to Eqn. (5), the asymptotic decay of the intra gap bound states at large distances from the impurity is governed by $g_0^2(r, \omega_0)$ and $g_1^2(r, \omega_0)$. Neglecting high-energy cut-off related oscillations at this length scale, one may extend the momentum space integrals in Eqn. (2) to infinity. This yields modified Bessel functions, i.e. $g_0(r, \omega_0) = -\frac{1}{W^2}\text{K}(0, r\sqrt{\Delta^2 - \omega_0^2}/v_f)$ and $g_1(r, \omega_0) = -\frac{i\sqrt{\Delta^2 - \omega_0^2}}{W^2}\text{K}(1, r\sqrt{\Delta^2 - \omega_0^2}/v_f)$. Therefore the wavefunctions of the impurity states decay as

$$\delta N_{\downarrow\uparrow}(r, \pm\omega_0) \propto r^{-1}e^{-2r\sqrt{\Delta^2 - \omega_0^2}/v_f}. \quad (6)$$

As Fig. 3 (left) shows, impurity states in the gap give rise to prominent features in future STM experiments: The density of the impurity state at the impurity site at $r = 0$ as well as the maximum of the density are strongly sensitive to the particular type of impurity. In general, impurity states with energies in the middle of the gap ($V_1 = 5W$ in Fig. 3 (left)) give rise to the sharpest maxima in the r-dependent LDOS. The ratio of the maximum density to the density at the impurity site increases with the potential strength V_1.

The ringstructure corresponding to these impurity states in STM images may give a powerful experimental tool for identifying particular impurities present in superconducting graphene. This is in contrast to the normal state graphene, where weak impurities do not give rise to resonances near the Dirac point and will therefore hardly be apparent in scanning tunneling spectroscopy (STS)[8].

In the continuum, Eqn. (5) encodes the real space shape of VBS and Friedel oscillations around the impurities. As Fig. 3 (right) shows exemplarily for a scalar impurity, the wavelength λ of these oscillations is in any case determined by the energy ω and the gap Δ: $\lambda = \pi v_f/\sqrt{\omega^2 - \Delta^2}$. Besides these oscillations giving rise to standing wave patterns in future STM exper-
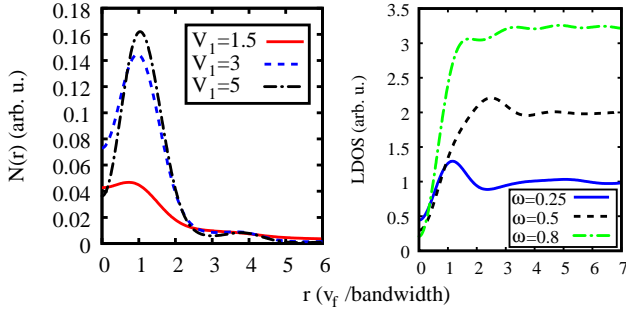
Figure 3: (Color online) Left panel: Density N of the intra-gap bound states as a function of the distance r from the impurity for purely magnetic scalar impurities and different potentials V_1. The impurity strength is given in units of the bandwidth W. Right panel: Friedel oscillations in the local density of states (LDOS) around a scalar impurity at $r = 0$ with $V_0 = 0$ and $V_1 = 3W$. The different curves correspond to the energies $\omega = 0.8$, 0.5 and $0.25W$. In both panels, the gap-parameter is $\Delta = W/10$.
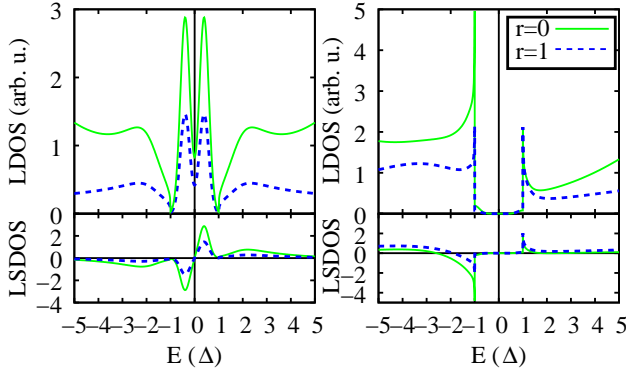

Figure 4: (Color online) The local density of states (LDOS, upper panel) and the local spin density of states (LSDOS, lower panel), $\delta N_\uparrow(r,\omega) - \delta N_\uparrow(r,\omega)$, at $r = 0$ and $r = 1$ is shown for scalar of impurities with different potentials: a purely magnetic impurity with $V_0 = 0$ and $V_1 = 3W$ (left) as well as an impurity with $V_0 = 2W$ and $V_1 = 1W$.

iments, certain resonances due to VBS will be an even more prominent as well as impurity specific feature in these experiments: The LDOS in Fig. 3 (right) exhibits a characteristic peak at $r \approx 1$ and $\omega \approx 0.25W$.

So far, we have discussed the r-dependent LDOS for different impurities and at different energies corresponding to STM images at fixed bias. The impurities will manifest themselves also in the energy dependence of the LDOS at fixed position, which is accessible by STS. In Fig. 4, the LDOS near a purely magnetic scalar impurity with $V_0 = 0$ and $V_1 = 3W$ is compared to an impurity contributing an electrostatic potential $V_0 = 2W$ and $V_1 = 1W$. The purely magnetic impurity, Fig. 4 (left), does not break particle hole symmetry and yields therefore a fully symmetric LDOS and a fully antisymmetric local spin density of states (LSDOS). This is in contrast to the more general second impurity, Fig. 4 (right), where

the LDOS and LSDOS are not symmetric under particle hole transformation. Therefore, the degree of symmetry of the local spectra allows to estimate, whether the impurity potential is magnetic or not - even in a non-spin polarized scanning tunneling spectroscopy experiment.

In *conclusion*, we argued that magnetic scattering will produce impurity induced bound and virtual bound states in superconducting graphene. These impurity states are similar to the Yu Lu-Shiba-Rusinov states in s-wave superconductors [9] and exhibit an intricate real space and particle-hole dependent structure. We discussed the energy dependence of these states as a function of the potential parameters and pointed out characteristic oscillation pattern as well as decay properties in real space. This spectroscopic and topographic information can be obtained by STM [14]. We showed that each impurity generates a specific signature in the real space LDOS and provided a guideline for identifying different impurities in future experiments. Since the Cooper pairs have zero momentum we find superconducting state in graphene to be a nontrivial example of valleytronics where valley quantum numbers are important [13].

[*] avb@lanl.gov, http://theory.lanl.gov
[1] K. S. Novoselov et al., Science **306**, 666 (2004).
[2] K. S. Novoselov et al., Nature **438**, 197 (2005).
[3] Y. Zhang et al., Nature **438**, 201 (2005).
[4] C. Bena and S. A. Kivelson, Phys. Rev. B **72**, 125432 (2005).
[5] N. M. R. Peres et al., Phys. Rev. B **73**, 125411 (2006).
[6] Y. V. Skrypnyk and V. M. Loktev, Phys. Rev. B **73**, 241402 (R) (2006).
[7] V. V. Cheianov and V. I. Fal'ko, Phys. Rev. Lett. **97**, 226801 (2006).
[8] T. O. Wehling et al., Phys. Rev. B **75**, 125425 (2007).
[9] A. V. Balatsky et al., Rev. Mod. Phys. **78**, 373 (2006).
[10] V. M. Pereira et al., Phys. Rev. Lett. **96**, 036801 (2006).
[11] H. B. Heersche et al., Nature **446**, 56 (2007).
[12] M. Titov and C. W. J. Beenakker, Phys. Rev. B **74**, 041401(R) (2006).
[13] A. Rycerz et al., Nature Phys. **3**, 172 (2007).
[14] A. Yazdani et al., Science **275**, 1767 (1997).
[15] C. Berger et al., Science **312**, 1191 (2006).
[16] P. Mallet et al., *Electron states of mono- and bilayer graphene on SiC probed by STM* (2007), cond-mat/0702406.
[17] C. W. J. Beenakker, Phys. Rev. Lett. **97**, 067007 (2006).
[18] T. O. Wehling and A. V. Balatsky (2007), (unpublished).